Insulin Prevents Depolarization of the Mitochondrial Inner Membrane in Sensory Neurons of Type 1 Diabetic Rats in the Presence of Sustained Hyperglycemia

Tze-Jen Huang,[1] Sally A. Price,[1] Lucy Chilton,[1] Nigel A. Calcutt,[2] David R. Tomlinson,[1] Alex Verkhratsky,[1] and Paul Fernyhough[1]

Mitochondrial dysfunction has been proposed as a mediator of neurodegeneration in diabetes complications. The aim of this study was to determine whether deficits in insulin-dependent neurotrophic support contributed to depolarization of the mitochondrial membrane in sensory neurons of streptozocin (STZ)-induced diabetic rats. Whole cell fluorescent video imaging using rhodamine 123 (R123) was used to monitor mitochondrial inner membrane potential ($\Delta\psi_m$). Treatment of cultured dorsal root ganglia (DRG) sensory neurons from normal adult rats for up to 1 day with 50 mmol/l glucose had no effect; however, 1.0 nmol/l insulin increased $\Delta\psi_m$ by 100% ($P < 0.05$). To determine the role of insulin in vivo, STZ-induced diabetic animals were treated with background insulin and the $\Delta\psi_m$ of DRG sensory neurons was analyzed. Insulin therapy in STZ-induced diabetic rats had no effect on raised glycated hemoglobin or sciatic nerve polyol levels, confirming that hyperglycemia was unaffected. However, insulin treatment significantly normalized diabetes-induced deficits in sensory and motor nerve conduction velocity ($P < 0.05$). In acutely isolated DRG sensory neurons from insulin-treated STZ animals, the diabetes-related depolarization of the $\Delta\psi_m$ was corrected ($P < 0.05$). The results demonstrate that loss of insulin-dependent neurotrophic support may contribute to mitochondrial membrane depolarization in sensory neurons in diabetic neuropathy. *Diabetes* 52:2129–2136, 2003

Mitochondrial dysfunction has been proposed as a central mediator of neurodegeneration in the central and peripheral nervous systems (1) and has been discussed as a critical modulator of diabetes complications in neurons (2) and endothelial cells (3). In the peripheral nerves of humans with diabetes, there is mitochondrial ballooning and disruption of internal cristae, although this is localized to Schwann cells and is rarely observed in axons (4). Similar structural abnormalities in mitochondria have been described in Schwann cells of galactose-fed rats (4) and in dorsal root ganglion (DRG) neurons of long-term streptozocin (STZ)-induced diabetic rats (2). Furthermore, acutely isolated adult sensory neurons from STZ-induced diabetic rats exhibit depolarization of the mitochondrial inner membrane (5). One current hypothesis is that high glucose concentrations induce elevated levels of oxidative phosphorylation, resulting in damaging amounts of reactive oxygen species (ROS)—the latter then mediate degenerative changes in mitochondrial structure and cell function (3).

A variety of hyperglycemia-induced secondary metabolic defects have been identified as possible causal factors in the etiology of the symmetrical sensory polyneuropathy observed in diabetes. These include polyol pathway flux (6), protein glycosylation (7), oxidative stress (8), and impaired neurotrophic support (9). Insulin and IGF-I and -II are trophic factors for embryonic (10) and adult sensory neurons (11) and modulate axon outgrowth and expression of cytoskeletal proteins (12,13). Trigeminal sensory ganglia exhibit high-affinity binding sites for insulin (14), and there is transcript expression for the insulin receptor and protein expression of the β-subunit in adult DRG (15). Deficits in insulin and IGF-dependent neurotrophic support have been proposed as key mediators of neurodegeneration in diabetes (16). IGF-I and -II can improve rates of peripheral nerve regeneration in normal (17,18) and STZ-induced diabetic animals and reverse diabetes-induced hyperalgesia (19). In humans, the local application of insulin can enhance nerve recovery in carpal tunnel syndrome in patients with type 2 diabetes (20). Finally, local injection or intrathecal delivery of insulin can prevent deficits in sensory and motor nerve conduction velocity (SNCV and MNCV) in STZ-induced diabetic rats independently of correction of hyperglycemia, implying a direct action on the sensory neuron (21,22).

Insulin and IGFs mediate growth and survival responses in neurons and non-neurons, in part, through phosphoinositide (PI) 3-kinase–dependent regulation of protein kinase B (PKB or Akt) (23–25). Activation of PKB has been shown to promote neuronal cell survival by growth factors against several apoptotic stimuli through modulation of Bcl-2 protein activity and subsequent modulation of mitochondrial function (24–26). In neurons, the loss of neu-

From the [1]School of Biological Sciences, University of Manchester, Manchester, U.K.; and the [2]Department of Pathology, University of California–San Diego, La Jolla, California.

Address correspondence and reprint requests to Dr. Paul Fernyhough, 1.124 Stopford Building, School of Biological Sciences, University of Manchester, Manchester, M13 9PT, U.K. E-mail:paul.fernyhough@man.ac.uk.

Received for publication 25 March 2003 and accepted in revised form 12 May 2003.

CCCP, carbonyl cyanide m-chlorophenylhydrazone; CREB, cAMP response element binding protein; DRG, dorsal root ganglia; FITC, fluorescein isothiocyanate, IR, insulin receptor; $\Delta\psi_m$, mitochondrial inner membrane potential; MNCV, motor nerve conduction velocity; NCV, nerve conduction velocity; PI, phosphoinositide; PKB, protein kinase B; R123, rhodamine 123; ROS, reactive oxygen species; SNCV, sensory NCV; STZ, streptozocin.

rotrophic support induces translocation of proapoptotic members of the Bcl-2 family of proteins, such as Bax, to the mitochondrial outer membrane and is a key neurodegenerative event in embryonic and mature neurons involving mitochondrial membrane depolarization and cytochrome C release (27,28).

The aim of this study was to determine whether mitochondrial dysfunction in the sensory neurons of diabetic rats was the result of a lack of insulin-dependent neurotrophic support and/or due to hyperglycemia. Single cell fluorescence video-imaging microscopy was used to semiquantitatively assess mitochondrial membrane potential, and the effects of insulin on this parameter in vitro and in vivo were investigated.

RESEARCH DESIGN AND METHODS

Induction of diabetes and insulin treatment. Male Wistar rats (300 g) were made diabetic by a single intraperitoneal injection of STZ (55 mg/kg; Sigma). Age-matched control groups were also created. Tail blood glucose was assayed 3 days after injection using glucose test strips (BM-Accutest; Roche Diagnostics, Basel, Switzerland) to confirm diabetes, and the animals were tested weekly thereafter. All diabetic and insulin-treated diabetic animals had blood glucose values >30 mmol/l. Rats were maintained for 8 weeks with free access to water and food. One group of STZ-induced diabetic animals received one-half of an insulin implant (LinPlant; LinShin, Scarborough, Canada) in the first week.

MNCV and SNCV measurement. Nerve conduction velocities (NCVs) were measured by subtraction of distal latencies for M-waves (for MNCV) and H-reflexes (for SNCV) elicited by stimulation at the sciatic notch and Achilles tendon. The principles and practicalities of these methods are described in detail elsewhere (29). In the present investigation, the measurements were performed on rats under isofluorane anesthesia and the measurement of NCV was accomplished within 5 min of the animal becoming unconscious; this is significantly faster than that described in our previously published study and may explain the higher NCVs produced in the present study (29). Core body temperature was monitored by a rectal probe and maintained at ~37°C. The temperature adjacent to the sciatic nerve was monitored by microthermocouple connected to an electronic thermometer (Comark Electronics, Sussex, U.K.). The upper flank of the animal was warmed using an infrared lamp to bring the near-nerve temperature to 37°C at the time of recording action potentials. The procedure is approved as part of the U.K. Home Office Project License awarded to D.R.T.

Glycated hemoglobin assay (HbA_1). Animals were exsanguinated postmortem in accordance with U.K. Home Office regulations and whole blood collected in sodium heparin-coated vacutainers (Becton Dickinson Vacutainer Systems, Oxford, U.K.). Glycated hemoglobin was separated from the unglycated form using an affinity column kit (441-B; Sigma-Aldrich, Poole, U.K.). Spectrophotometric analysis at 415 nm measured the percentage of glycated hemoglobin compared with total hemoglobin.

Sciatic nerve polyol measurements. Sciatic nerves were frozen and stored at −70°C. Sugars and polyols were extracted from freeze-dried nerves by boiling for 15 min in a solution of distilled water and 30 μg α-methylmannoside to act as an internal standard. Trimethylsilyl derivatives of the extracted nerve sugars and internal standard were produced and assayed by gas chromatography using a Hewlett Packard (Avondale, PA) 5890A gas chromatograph fitted with an Ultra 1 capillary column and a flame ionization detector.

Sensory neuron cultures. Sensory neurons from DRG of adult rats were isolated and dissociated using a previously described method (11). The cells were plated onto poly-L-ornithine-laminin–coated 1.1-cm glass coverslips in serum- and insulin-free F12 medium (Life Technologies, Paisley, U.K.) in the presence of modified N2 additives (containing no insulin) at 37°C in a 95% air/5% CO_2 humidified incubator. Lumbar DRG sensory neurons from treated animals were cultured for 3–4 h and then assessed for mitochondrial function. For in vitro experiments, sensory neurons were cultured for up to 24 h with or without insulin (1.0 or 10 nmol/l) or 50 mmol/l glucose, and then mitochondrial inner membrane potential ($\Delta\psi_m$) was assessed.

$\Delta\psi_m$ and intracellular calcium measurements using rhodamine 123 and fura-2/AM. This technique was based on previously described procedures (1,30,31). Cultured DRG sensory neurons were loaded with 10 μmol/l rhodamine 123 (R123) (for mitochondrial analysis) and/or fura-2/AM (for calcium) for 10 min at room temperature in standard physiological saline (in mmol/l): 140 NaCl, 3 KCl, 2 $CaCl_2$, 2 $MgCl_2$, 10 glucose, and 20 HEPES/NaOH, pH 7.4. After loading, the cells were washed in normal saline for an additional 30 min to ensure the de-esterification of R123. Glass coverslips with stained cells were transferred into the 500-μl perfusion chamber mounted on the stage of an upright microscope (BX50WI; Olympus, Tokyo, Japan) equipped with 20× water immersion objectives. Neurons were exposed to excitation light provided by a monochromator (Polychrom IV; TILL Photonics, Gräfelfing, Germany) at 490 nm (for R123) and 340 and 380 nm (for fura-2/AM). Emitted fluorescent light was collected at 530 ± 15 nm (for R123 and fura-2/AM) by a frame-transfer, cooled, intensified, charge-coupled device camera (Gene IV; Roper Scientific, Marlow, U.K.). The imaging data were acquired and analyzed using MetaFluor/MetaMorph software (Universal Imaging, West Chester, PA). The fura-2/AM signal was calibrated using an ionomycin-based in situ proce-

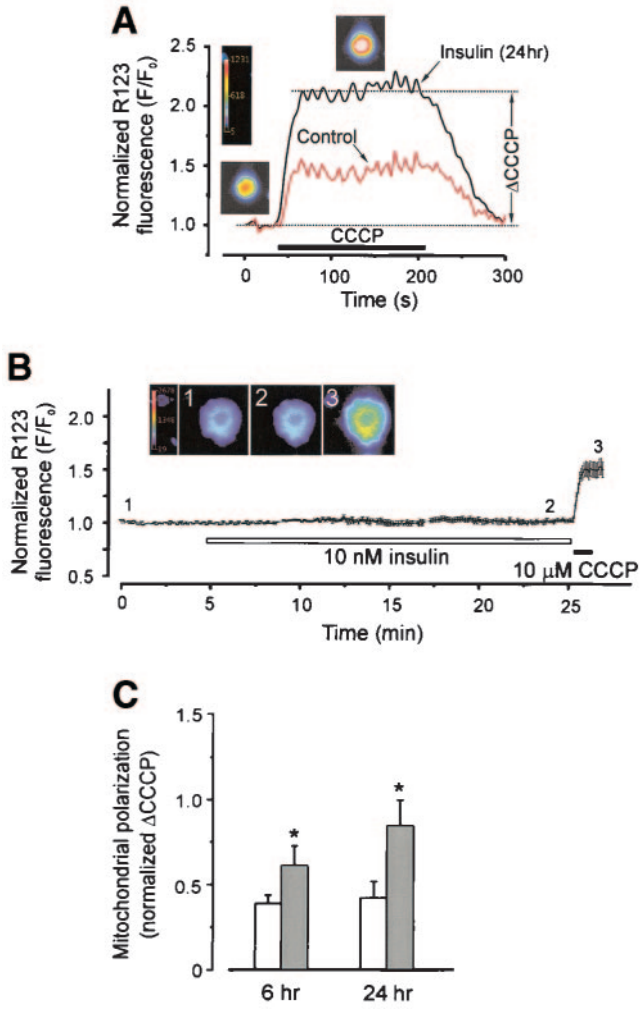

FIG. 1. Insulin modulates $\Delta\psi_m$ in cultured adult sensory neurons. *A*: Demonstration of the technique used for semiquantitatively deriving a whole cell value for $\Delta\psi_m$ from the neuronal soma. For each cell, the baseline R123 fluorescence (resting fluorescence at time 0) was normalized to 1 [termed F_0, relatively low fluorescence; see insert (1)], and then the increase in R123 fluorescence in response to 10 μmol/l CCCP-induced membrane depolarization was measured [termed F, high fluorescence level; see insert (2)]. The ratio of F to F_0, therefore, provides a semiquantitative measure of the relative increase in R123 fluorescence intensity upon complete mitochondrial depolarization. The resulting ΔCCCP value was, therefore, directly proportional to the summed polarization status of the mitochondrial inner membrane of all mitochondria within the neuronal soma. *B*: Control DRG sensory neurons were treated acutely with 10 nmol/l insulin for ≤20 min. The normalized R123 fluorescence intensity is presented. Inserts 1–3 illustrate the R123 fluorescence signals at specific time points; insert 3 depicts the highest level of R123 fluorescence following CCCP-induced depolarization (means ± SE, n = 21 neurons). *C*: Sensory neuron cultures were treated for 6 or 24 h with and without 1.0 nmol/l insulin and mitochondrial polarization status calculated. □, control; ■, insulin. *P < 0.05 vs. control (means ± SE, n = 39–43 neurons).

dure (32); the parameters R_{min}, R_{max}, and K* were 0.2, 1.0, and 451 nmol/l, respectively.

Figure 1*A* shows the semiquantitative R123–based technique used to assess $\Delta\psi_m$. Carbonyl cyanide m-chlorophenylhydrazone (CCCP), an uncoupler (or protonophore), was used to collapse the proton gradient and inner membrane potential across the mitochondrial inner membrane. Collapse of mitochondrial membrane potential by application of 10 μmol/l CCCP caused an increase in R123 fluorescence due to unquenching and the release of R123 from the mitochondrial matrix into the cytosol. This elevated fluorescence intensity was then normalized to the baseline level of fluorescence before CCCP treatment (F_0).

NAD(P)H autofluorescence measurement. Real-time NAD(P)H autofluorescence [a relative indicator of NAD(P)H redox state] was measured at an excitation wavelength of 340 nm, and autofluorescence was collected at 510 ± 15 nm from single neurons. Fluorescence changes were expressed as F/F_0, where F is the autofluorescence at any given time and F_0 is the initial autofluorescence. $\Delta F/F_0$ CCCP is the maximal response of fluorescence due to the addition of CCCP and is used to semiquantify the relative NAD(P)H level associated with the mitochondria of a single neuron. There are significant limitations to this technique. For example, while the major autofluorescence signal derives from NAD/NADH associated with the mitochondria (as much as 80–90% of the total fluorescence) (33), there is the possibility of alterations in NADP/NADPH levels in the cytoplasm impacting the fluorescence level.

Western blotting and immunocytochemistry for insulin receptors. Cultured DRG neurons were harvested with homogenization buffer (50 mmol/l Tris-HCl, pH 7.4, 1% NP-40, 0.25% sodium deoxycholate; 150 mmol/l NaCl, 1 mmol/l EGTA, 1 mmol/l phenylmethylsulfonyl fluoride, 1 μmol/ml each aprotinin, leupeptin, and pepstatin, 1 mmol/l Na_3VO_4, and 1 mmol/l NaF), and 30 μl Laemmli sample buffer was added. Total protein (5 μg) was subjected to SDS-PAGE and then transferred to nitrocellulose, which was then incubated with primary antibody (anti–insulin receptor-α, 1:500 [Santa Cruz Biotech] and anti–insulin receptor-β, 1:250 [BD Transduction]) in 3% milk PBS overnight at 4°C, followed by incubation of secondary antibody (horseradish peroxidase–conjugated anti-rabbit secondary antibody, 1:2,500 [Cell Signaling]) at room temperature for 1 h. Enhanced chemiluminescence (LumiGlu; Cell Signaling) was used to detect the signal from the blot.

For immunocytochemistry, cultured DRG neurons were fixed with ice-cold 4% paraformaldehyde (in 0.1 mol/l phosphate buffer, pH 7.4) for 30 min at 4°C followed by permeabilizing with 1% Triton X-100 in PBS for 30 min. Nonspecific binding was blocked by the incubation of 10% donkey serum for 1 h at room temperature and washed three times with PBS for 15 min. Fixed cells were then incubated with anti–insulin receptor-β antibody (1:100; BD Transduction) overnight in a humidified chamber followed by fluorescein isothiocyanate (FITC)-conjugated secondary antibody (1:200) for 1 h at room temperature. Fluorescence was examined using Leica fluorescence microscopy equipped with FITC and DAPI filters.

Data analysis. Where appropriate, data were subjected to one-way ANOVA using the Statistical Package for Social Scientists (SPSS/PC+; SPSS, Chicago, IL). Where the *F* ratio gave $P < 0.05$, comparisons between individual group means were made by Scheffe's multiple range test at a significance level of $P = 0.05$. In all other situations, a standard Student's *t* test was used for single comparisons.

RESULTS

Cultured sensory neurons express insulin receptors. We first confirmed that cultured adult sensory neurons expressed receptors for insulin. Figure 2*A* shows that cultured DRG neurons express insulin receptor (IR) subunits-α (IRα) and -β (IRβ). The molecular weight of the IRα subunit (~135 kDa) confirms that this receptor is of the peripheral type, with a higher molecular weight than the corresponding receptor found in the adult brain. Immunocytochemical labeling for IRβ confirmed a neuronal localization with strong staining of the plasma membrane (Fig. 2*B*).

Insulin enhances $\Delta\psi_m$ in cultured DRG sensory neurons. Dissociated adult rat DRG sensory neurons from normal animals were cultured for up to 24 h with insulin, and the effect on $\Delta\psi_m$ was analyzed using R123 fluorescence and the CCCP-dependent collapse of the mitochondrial membrane potential (Fig. 1*A* for method). Acute treatment with 10 nmol/l insulin (≤20 min) had no effect

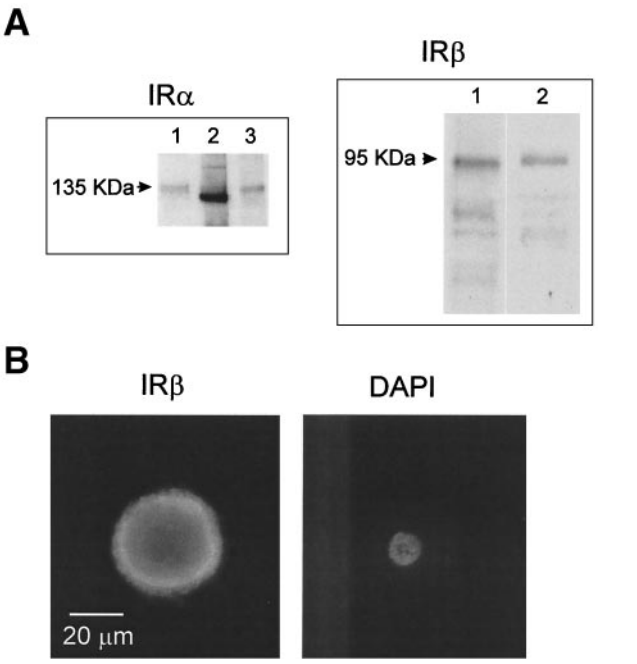

FIG. 2. Cultured DRG sensory neurons express IR subunits. *A*: Western blots are presented, showing signals for IR subunits-α (IRα) and -β (IRβ) in adult liver (*lane 1*), adult brain (*lane 2* and IRα), and cultured DRG neurons (*lane 3* for IRα; *lane 2* for IRB). *B*: Immunocytochemical staining for IRβ is presented in a single adult sensory neuron. DAPI staining indicates that this is a single large neuron. Bar = 20 μm.

on R123 fluorescence intensity (normalized) (Fig. 1*B*). Treatment with 1.0 nmol/l insulin for 6 or 24 h significantly raised the $\Delta\psi_m$ (as determined using the normalized amplitude of CCCP-induced increase in R123 fluorescence) by ~50 and 100%, respectively ($P < 0.05$ for both; Fig. 1*C*). In all insulin treatment studies there were no changes in neuron survival during the period of study (in the presence or absence of insulin, data not shown).

High glucose concentration does not affect mitochondrial function in cultured sensory neurons. In an attempt to mimic hyperglycemia, the cultures were treated with a high concentration of glucose (50 mmol/l). Acute treatment with 50 mmol/l glucose added to standard physiological saline for ≤20 min had only a fast transient effect on R123 fluorescence intensity and NAD(P)H autofluorescence levels (Fig. 3*A* and *B*). Over a period of 2–3 min, the glucose treatment caused a transient depolarization of the mitochondrial membrane that coincided with a similarly transient lowering of the NAD(P)H autofluorescence signal. The latter was most likely due to oxidation of NADH within the mitochondrion, but oxidation of NADPH within the cytoplasm cannot be ruled out. When we treated neurons with 50 mmol/l glucose with adjustment for alterations in osmolarity, no effect on R123 fluorescence was observed for ≤6 h during the continuous application of high glucose–containing solution (data not shown). Therefore, we conclude that rapid mitochondrial depolarization caused by constant treatment with 50 mmol/l glucose within the normal bathing saline solution resulted in hyperosmotic stress. Cultures were then continually treated with 50 mmol/l glucose in the presence or absence of 1.0 nmol/l insulin for 1 day (Fig. 3*D*). Constant treatment with insulin caused a significant 100% increase in $\Delta\psi_m$, while 50 mmol/l glucose was without effect.

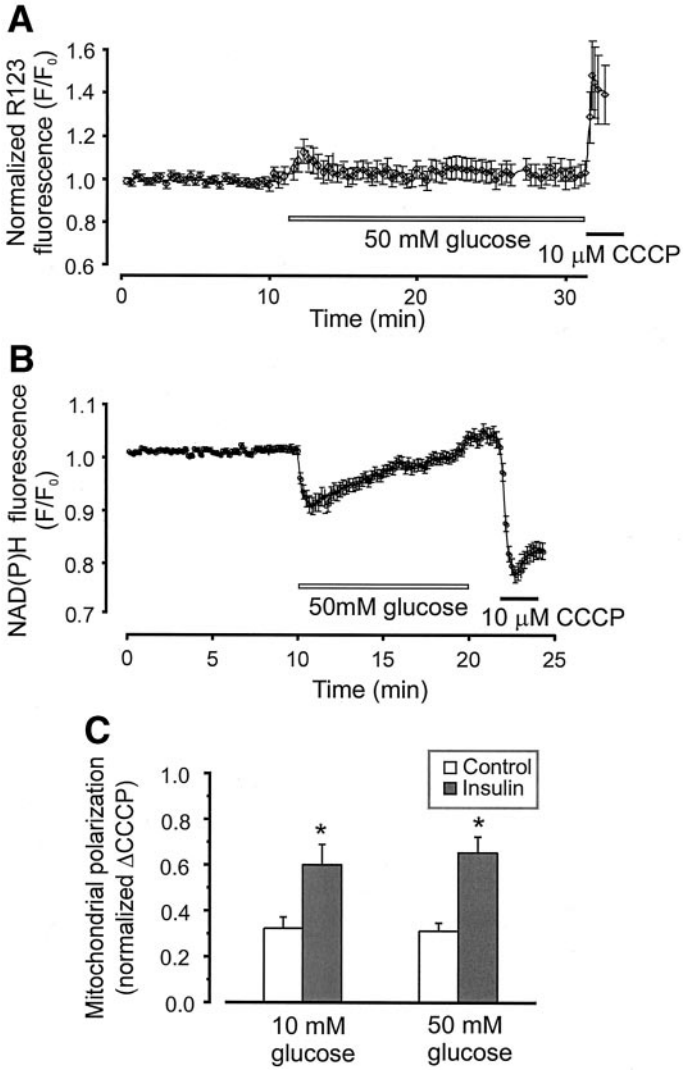

FIG. 3. High concentration of glucose has no impact on $\Delta\psi_m$ in sensory neurons. *A*: Sensory neuron cultures were treated acutely with 50 mmol/l glucose for ≤30 min and R123 fluorescence assessed (means ± SE, n = 18 neurons). *B*: The same treatment regimen was used, but NAD(P)H redox state was measured using autofluorescence (means ± SE, n = 16 neurons). *C*: Cultures were treated for 24 h with 10 or 50 mmol/l glucose and with and without 1.0 nmol/l insulin, and mitochondrial polarization was measured as previously described. *P < 0.05 vs. control (means ± SE; n = 25–32 neurons; t test) .

Background insulin therapy prevents deficits in nerve physiology but does not affect hyperglycemia or nerve polyol levels in STZ-induced diabetic rats. The results in Figs. 1 and 3 suggested that insulin, but not glucose, was a key regulator of mitochondrial function in vitro. An in vivo experiment was therefore designed in which STZ-induced diabetic rats were treated with suboptimal insulin concentrations that provided background insulin, albeit at a dose that did not affect hyperglycemia (Fig. 4*A* describes experimental design). A subgroup of STZ-induced diabetic rats received one-half (~1 unit/day) of an insulin implant (Linplant; Linshin) from week 1 onward. Figures 4*B* and *C* show that the insulin therapy raised the total body weight of STZ-induced diabetic animals by ~50 g over the 8-week duration of the study. At study end, the insulin-treated group had body weights ~150 g lower than those of the age-matched control animals. The insulin therapy regimen had no effect on blood glucose levels in STZ-induced diabetic rats, as measured using test strips (all STZ-induced diabetic and insulin-treated animals showed >25 mmol/l glucose; data not shown). Additionally, insulin treatment had no significant effect on the raised glycated hemoglobin levels in STZ-induced diabetic rats (Fig. 5*A*). Sciatic nerve polyol levels, including glucose, fructose, and sorbitol were all raised significantly in the STZ-induced diabetic group (Fig. 5*C*– *E*). Insulin therapy did not reduce the polyol accumulation; in fact, there was evidence that glucose and sorbitol levels were raised (Fig. 5*C* and *D*). For example, insulin treatment increased glucose levels in nerve to 41.6 ± 4.4 nmol/mg compared with 31.5 ± 9.6 in untreated STZ-induced diabetic animals ($P < 0.05$). Furthermore, insulin treatment approximately doubled sorbitol levels in nerve from 3.47 ± 1.33 nmol/mg in STZ-induced diabetic animals to 6.25 ± 2.33 nmol/mg in the treated group. Myoinositol levels were significantly reduced in the STZ-induced diabetic group, and insulin treatment had no effect (Fig. 5*B*). Finally, insulin treatment partially, although significantly, normalized the MNCV value ($P < 0.02$) and almost completely corrected the diabetes-induced deficit in the SNCV ($P < 0.02$; as measured using the H-reflex) (Fig. 4*D* and *E*).

Treatment of STZ-induced diabetic rats with background insulin normalizes $\Delta\psi_m$ in sensory neurons. Lumbar DRG from each animal group were acutely isolated and cultured, and $\Delta\psi_m$ was measured using R123 fluorescence as described above. Sensory neurons from STZ-induced diabetic animals had a 50% decrease in the level of the $\Delta\psi_m$ compared with age-matched control animals (Fig. 6*A* and *B*). Insulin treatment completely prevented the diabetes-induced deficit in $\Delta\psi_m$. Calcium homeostasis in neurons is intimately linked to mitochondrial function, therefore resting intracellular calcium was also analyzed; STZ-induced diabetes raised this parameter from ~100 to 175 nmol/l, and insulin treatment ameliorated this abnormality (Fig. 6*C*).

DISCUSSION

The results show that insulin can prevent diabetes-induced deficits in $\Delta\psi_m$ in adult DRG sensory neurons. These findings complement those of Srinivasan et al. (5), who first showed mitochondrial membrane depolarization in sensory neurons of STZ-induced diabetic rats. However, in the present study the effect of insulin in vivo was not mediated through normalization of hyperglycemia because the insulin concentration used was too low to significantly affect glucose metabolism. Measurement of glycated hemoglobin and sciatic nerve polyol levels confirmed that hyperglycemia in STZ-induced diabetic rats was not affected by the background insulin regimen. In vitro experiments on normal cultured DRG sensory neurons treated with 50 mmol/l glucose also showed no direct effect on $\Delta\psi_m$, whereas treatment with insulin significantly raised the $\Delta\psi_m$ by 100% (Figs. 1 and 3).

In the present study, the failure of glucose to induce mitochondrial depolarization in cultured adult sensory neurons contradicts a recent investigation (34). There are a number of methodological discrepancies that may account for this. First, Russell et al. (34) used embryonic sensory neurons that have different neurotrophic require-

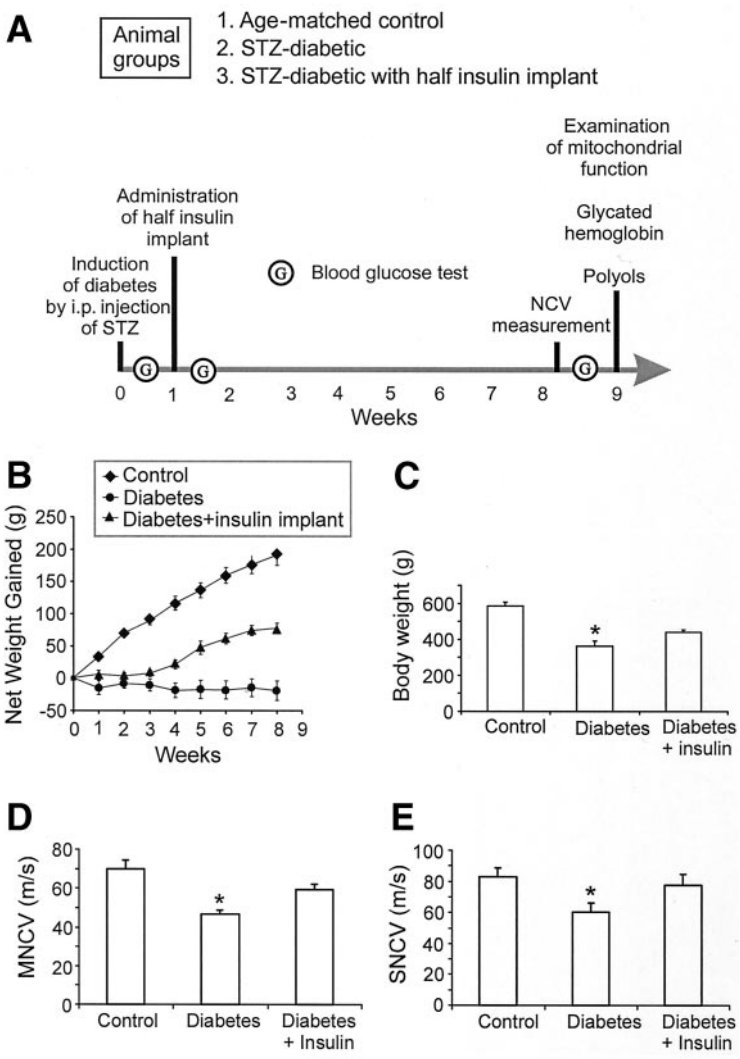

FIG. 4. Effect of background insulin treatment on body weight and NCV in STZ-induced diabetic animals. *A*: The experimental design of the in vivo study. *B*: The weekly body weight changes of the experimental groups. The diabetic animals were maintained for 8 weeks and a subgroup was treated with one-half of an insulin implant from 1 week onward. ◆, age-matched control; ●, animals with diabetes; ▲, animals with diabetes treated with insulin. *C*: The final body weights of the experimental groups. The MNCV (*D*) and SNCV (*E*) values are in meters per second. Values are means ± SE (n = 8–12 animals). *P < 0.02 for diabetes versus other groups (one-way ANOVA).

ments from the adult neurons used in the present study. Second, Russell et al. used a fluorimetric analysis of cell suspensions, which does not identify neuronal-specific signals, whereas our technique allows detection of neuron-specific signals. Their use of tetramethylrhodamine methylester may also impede interpretation, because when illuminated, tetramethylrhodamine methylester triggers opening of the permeability transition pore, generation of ROS, and release of apoptotic signals (35). In contrast, we used R123, which does not have this limitation under the conditions used in the present study. Finally, data obtained by the confocal imaging technique used by Russell et al. is also difficult to interpret because any alterations in plasma membrane potential, possibly induced by glucose, can impact the fluorescence signal emitted from the mitochondria (31). This is why we used single neuron imaging at the light microscope level. Any or all of the above might account for the discrepancies between the two studies and give us confidence in our methodology and findings.

The ability of insulin to prevent deficits in $\Delta\psi_m$ in sensory neurons in diabetes does suggest a role for this neurotrophic factor in the etiology of the mitochondrial depolarization observed; however, some caution must be exercised before discounting hyperglycemia completely. The in vitro studies only involved short-term exposure of neurons to high glucose concentrations. The study by Nishikawa et al. (3), which demonstrated high glucose–induced ROS production linked to excessive oxidative phosphorylation, involved the in vitro exposure of endothelial cells for at least 1 week. Unfortunately, such studies cannot be performed in adult sensory neurons because of the involvement of proliferating non-neurons at longer time points in culture. Therefore, a role for hyperglycemia in the etiology of mitochondrial dysfunction and cellular degeneration remains a possibility; however, what is clear is that insulin-dependent neurotrophic effects may also be involved in the pathogenesis and are certainly capable of inducing repair of mitochondrial abnormalities.

Circulating insulin is obviously downregulated in type 1 diabetes, and it has been determined that background levels fall significantly <1–4 nm in STZ-induced diabetic animals and in humans (16). DRG sensory neurons express receptors for insulin (14,15) (Fig. 2), and insulin does regulate neuronal phenotype (16). For example, insulin elevates axonal outgrowth in embryonic and adult sensory neurons (10,11), and in clonal cell lines, neurofilament and tubulin mRNA expression are enhanced in association with increased neurite elongation (12,13). Insulin mediates survival responses in neurons and non-neurons, in part, through phosphoinositide (PI) 3-kinase–

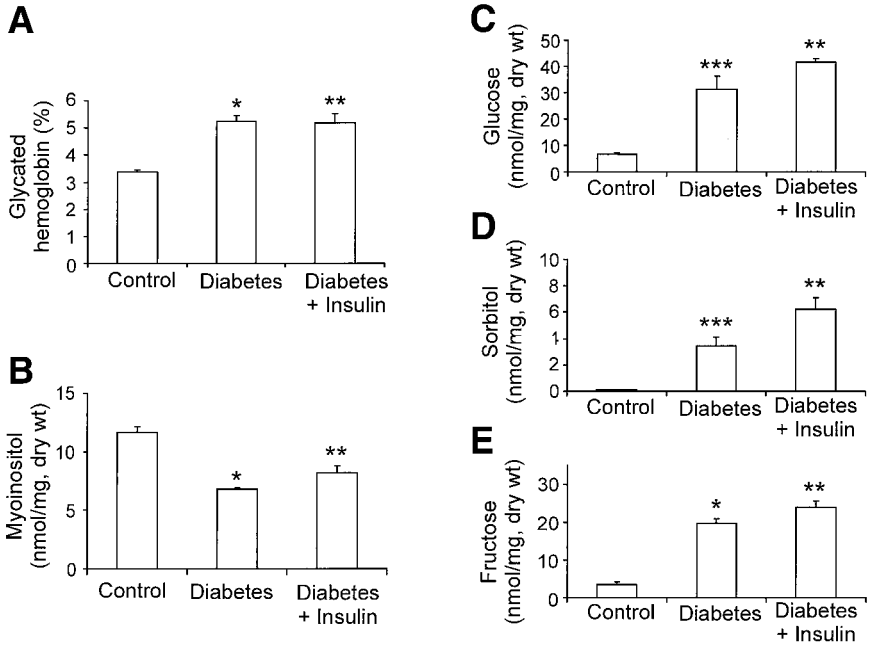

FIG. 5. Insulin treatment did not lower glycated hemoglobin or sciatic nerve polyol levels in STZ-induced diabetic animals. *A*: Glycated hemoglobin values (in percent). Values are means ± SE (n = 8–12). Myoinositol (*B*), glucose (*C*), sorbitol (*D*), and fructose (*E*) levels are in nanomoles per milligram dry weight of sciatic nerve. Values are means ± SE (n = 4–8 animals). *P < 0.01 for diabetes versus control; **P < 0.05 for diabetes + insulin versus control; ***P < 0.05 for diabetes versus diabetes + insulin (one-way ANOVA).

dependent regulation of protein kinase B (PKB or Akt) with associated modulation of mitochondrial function (23–25). PKB promotes neuronal cell survival by growth factors against several apoptotic stimuli through modulation of Bcl-2 protein function (24–26). In STZ-induced diabetic rats, impaired mitochondrial function is associated with reduced Bcl-2 expression (5), and in Schwann cells (26) exposed to high glucose the resulting degeneration is linked to impaired functioning of Bcl-xL. In Schwann cells, overexpression of Bcl-xL afforded protection to high glucose, as did treatment with IGF-I operating through a PI 3-kinase–dependent pathway (26). These important regulators of mammalian apoptosis function, in part, by altering mitochondrial function, through changes in permeability transition pore function (1). Furthermore, loss of neurotrophic support in neurons induces translocation of Bim and Bax to the mitochondrial outer membrane and is a key pro-apoptotic event in embryonic and mature neurons involving mitochondrial membrane depolarization and cytochrome C release (27,28). Thus, we hypothesize that Bax is one possible target for insulin signaling, and that its PI 3-kinase/Akt–regulated translocation may regulate $\Delta\psi_m$ in the absence of an effect on cell survival, since significant levels of sensory neuron cell death are not observed in cell culture in the absence of insulin (11) and/or presence of high glucose concentrations (36). Furthermore, in acute STZ-induced diabetes (2–3 months) there is no evidence of neuron loss in DRG (37), and this corresponds with maintenance of normal DRG neuron numbers in postmortem samples from patients with diabetes (38).

Apart from putative changes in expression/localization of Bcl-2 family proteins, the insulin-mediated effect on mitochondrial membrane potential could be regulated by

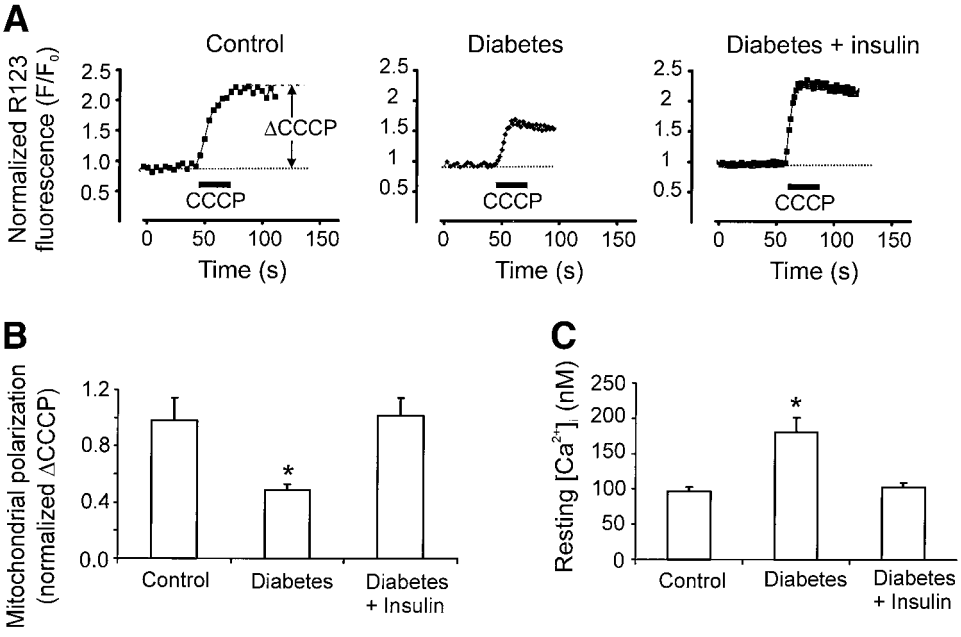

FIG. 6. Diabetes-induced mitochondrial dysfunction in sensory neurons was prevented by insulin treatment. *A*: Typical R123 fluorescence (normalized) traces of sensory neurons acutely isolated from animals that were age-matched controls, had diabetes, or had diabetes treated with insulin. *B*: The elevation in R123 fluorescence induced by CCCP is shown and was used to derive the values. The mitochondrial polarization status of the experimental groups is shown (*B*) as well as the resting intracellular calcium concentration (*C*). Values are means ± SE (n = 119–141 neurons). *P < 0.01 for diabetes versus control (one-way ANOVA); **P < 0.01 for diabetes + insulin versus diabetes (t test).

enhanced glucose transport, glucose metabolism, or alterations in electron transfer chain redox state. Insulin-dependent changes in glucose transport are unlikely because this process is not limiting in sensory neurons (39). This may be true for neurons, however the polyol data showing enhanced glucose, sorbitol, and fructose levels in the sciatic nerve (Fig. 5) suggest that the background insulin treatment may trigger enhanced glucose utilization in Schwann cells and other non-neurons located in the nerve fiber of STZ-induced diabetic rats. In addition, insulin is known to regulate glucose metabolism at both the posttranslational and transcriptional levels in liver, muscle, and fat tissues (40). At the posttranslational level, insulin directly controls the activities of a set of metabolic enzymes involved in gluconeogenesis and glycolysis (41). Insulin increases transcription of glycolytic enzymes such as glucokinase, pyruvate kinase, and acetyl-CoA carboxylase (42). These phenotype changes may have a significant impact on the levels of redox equivalents [e.g., NAD(P)H] that might directly affect the $\Delta\psi_m$ through an increase in electron donation. Also, modulation of mitochondrial function can also be mediated through alterations in the operation of the electron transfer chain. For example, the level of cytochrome C (a critical and possibly rate-limiting component within the electron transfer chain) can also be regulated through the cAMP response element binding protein (CREB) transcription factor upon serum stimulation (43,44). In fact, our preliminary data show that insulin activates CREB in cultured DRG neurons (T.-J.H., A.V., P.F., manuscript in preparation). Intriguingly, one-third of CREB-regulated genes (genes that contain CREB binding sites) are glucose metabolism related (including hexokinase and cytochrome C) (45).

Diabetes-induced alterations in calcium homeostasis may also underlie abnormalities in mitochondrial polarization status. Mitochondrial function is intimately associated with intracellular calcium homeostasis and calcium signaling. First, mitochondria provide ATP for numerous Ca^{2+} pumps responsible for regulation of resting $[Ca^{2+}]_i$ and Ca^{2+} removal from the cytoplasm (46). Second, mitochondria act as a dynamic calcium store, capable of buffering substantial Ca^{2+} loads and release accumulated Ca^{2+}, thus shaping cytoplasmic Ca^{2+} signals (47). In fact, in peripheral nerve of 5-month-old STZ-induced diabetic rats, the levels of Ca^{2+} in axoplasm and in mitochondria were significantly raised, as measured using electron probe X-ray microanalysis (48). Both ATP production and mitochondrial Ca^{2+} accumulation are directly controlled by $\Delta\psi_m$, and chronic mitochondrial depolarization may consequently affect Ca^{2+} homeostatic cascades. As we have demonstrated previously (30), STZ-induced diabetes considerably destabilizes Ca^{2+} homeostasis and Ca^{2+} signaling in sensory neurons, but most importantly, in vivo treatment with background insulin fully restores resting $[Ca^{2+}]_i$ (Fig. 6*C*). This effect of long-lasting insulin treatment could be extremely important in the context of diabetic neuropathies, as impaired cytosolic Ca^{2+} homeostasis has a well-documented role in various neurodegenerative disorders and neuronal death (49). Furthermore, limited ATP production in diabetes may affect Ca^{2+} homeostasis within the endoplasmic reticulum, which may in turn significantly contribute to the development of neuropathic changes (50).

In vitro sensory neurons are quiescent but do not die in the absence of insulin, while enhanced insulin signaling could optimize mitochondrial function and, presumably, increase ATP production, thereby maintaining synthetic processes. The depolarization of the neuronal mitochondrial membrane in diabetes will result in a corresponding decrease in the driving force for ATP production. Energy status in the sciatic nerve of STZ-induced diabetic rats is compromised (51). Obrosova et al. (51) have shown that although levels of ATP were not significantly altered (a 20% decrease was observed) in the sciatic nerve of STZ-induced diabetic rats, there was a significant reduction in the levels of stored high-energy phosphates, such as phosphocreatine (51). Diabetic neuropathy is characterized by a range of alterations in sensory neuron gene expression and an impaired regenerative response in the event of peripheral axon damage (9). Additionally, slow axonal transport of a range of axoplasmic materials, including neurofilaments, is impaired (52,53). All of these aspects of neuropathic pathology have a common requirement for energy, mainly in the form of ATP, and clearly, if mitochondrial function is impaired, considerable detriment to the neuron will result.

In summary, the results show that a lack of insulin-dependent neurotrophic support may underlie mitochondrial dysfunction in sensory neurons in diabetic neuropathy. While we cannot be certain of an involvement of loss of insulin in the etiology of mitochondrial dysfunction, the results show that therapy with insulin can correct diabetes-induced disturbances in mitochondrial function. It can be proposed that such a decrease in mitochondrial membrane polarization will impact a plethora of sensory neuron functions through a decrease in available energy (ATP and/or other stores) and may be a critical component of the etiology of diabetic sensory polyneuropathy.

ACKNOWLEDGMENTS

This work was funded by grants from the Juvenile Diabetes Research Foundation (to P.F.), from Diabetes U.K. (to P.F. and A.V.), and from the Medical Research Council (to D.R.T.). T.-J.H. was a recipient of an Overseas Research Scholarship.

REFERENCES

1. Nicholls DG, Budd SL: Mitochondria and neuronal survival. *Physiol Rev* 80:315–360, 2000
2. Sasaki H, Schmelzer JD, Zollman PJ, Low PA: Neuropathology and blood flow of nerve, spinal roots and dorsal root ganglia in longstanding diabetic rats. *Acta Neuropathol* 93:118–128, 1997
3. Nishikawa T, Edelstein D, Du XL, Yamagishi S, Matsumura T, Kaneda Y, Yorek MA, Beebe D, Oates PJ, Hammes HP, Giardino I, Brownlee M: Normalizing mitochondrial superoxide production blocks three pathways of hyperglycaemic damage. *Nature* 404:787–790, 2000
4. Kalichman MW, Powell HC, Mizisin AP: Reactive, degenerative, and proliferative Schwann cell responses in experimental galactose and human diabetic neuropathy. *Acta Neuropathol* 95:47–56, 1998
5. Srinivasan S, Stevens M, Wiley JW: Diabetic peripheral neuropathy: evidence for apoptosis and associated mitochondrial dysfunction. *Diabetes* 49:1932–1938, 2000
6. Tomlinson DR, Willars GB, Carrington AL: Aldose reductase inhibitors and diabetic complications. *Pharmacol Ther* 54:151–194, 1992
7. Brownlee M: Lilly Lecture 1993: glycation and diabetic complications. *Diabetes* 43:836–841, 1994

8. Van Dam PS, Bravenboer B: Oxidative stress and antioxidant treatment in diabetic neuropathy. *Neurosci Res Commun* 21:41–48, 1997
9. Fernyhough P, Tomlinson DR: The therapeutic potential of neurotrophins for the treatment of diabetic neuropathy. *Diabetes Reviews* 7:300–311, 1999
10. Recio-Pinto E, Rechler MM, Ishii DN: Effects of insulin, insulin-like growth factor-II, and nerve growth factor on neurite formation and survival in cultured sympathetic and sensory neurons. *J Neurosci* 6:1211–1219, 1986
11. Fernyhough P, Willars GB, Lindsay RM, Tomlinson DR: Insulin and insulin-like growth factor I enhance regeneration in cultured adult rat sensory neurones. *Brain Res* 607:117–124, 1993
12. Wang C, Li Y, Wible B, Angelides KJ, Ishii DN: Effects of insulin and insulin-like growth factors on neurofilament mRNA and tubulin mRNA content in human neuroblastoma SH-SY5Y cells. *Brain Res Mol Brain Res* 13:289–300, 1992
13. Fernyhough P, Mill JF, Roberts JL, Ishii DN: Stabilization of tubulin mRNAs by insulin and insulin-like growth factor I during neurite formation. *Brain Res Mol Brain Res* 6:109–120, 1989
14. Waldbillig RJ, LeRoith D: Insulin receptors in the peripheral nervous system: a structural and functional analysis. *Brain Res* 409:215–220, 1987
15. Sugimoto K, Murakawa Y, Sima AA: Expression and localization of insulin receptor in rat dorsal root ganglion and spinal cord. *J Peripher Nerv Syst* 7:44–53, 2002
16. Ishii DN: Implication of insulin-like growth factors in the pathogenesis of diabetic neuropathy. *Brain Res Brain Res Rev* 20:47–67, 1995
17. Glazner GW, Lupien S, Miller JA, Ishii DN: Insulin-like growth factor II increases the rate of sciatic nerve regeneration in rats. *Neuroscience* 54:791–797, 1993
18. Kanje M, Skottner A, Sjoberg J, Lundborg G: Insulin-like growth factor I (IGF-I) stimulates regeneration of the rat sciatic nerve. *Brain Res* 486: 396–398, 1989
19. Zhuang HX, Wuarin L, Fei ZJ, Ishii DN: Insulin-like growth factor (IGF) gene expression is reduced in neural tissues and liver from rats with non-insulin-dependent diabetes mellitus, and IGF treatment ameliorates diabetic neuropathy. *J Pharmacol Exp Ther* 283:366–374, 1997
20. Ozkul Y, Sabuncu T, Yazgan P, Nazligul Y: Local insulin injection improves median nerve regeneration in NIDDM patients with carpal tunnel syndrome. *Eur J Neurol* 8:329–334, 2001
21. Singhal A, Cheng C, Sun H, Zochodne DW: Near nerve local insulin prevents conduction slowing in experimental diabetes. *Brain Res* 763:209–214, 1997
22. Brussee V, Buchan AM, Zochodne DW: Do insulin and IGF-1 target neurons in experimental diabetes? *Society for Neuroscience Annual Meeting*, San Diego, CA, 2–7 November 2001
23. Dudek H, Datta SR, Franke TF, Birnbaum MJ, Yao R, Cooper GM, Segal RA, Kaplan DR, Greenberg ME: Regulation of neuronal survival by the serine-threonine protein kinase Akt. *Science* 275:661–665, 1997
24. Orike N, Middleton G, Borthwick E, Buchman V, Cowen T, Davies AM: Role of PI 3-kinase, Akt and Bcl-2-related proteins in sustaining the survival of neurotrophic factor-independent adult sympathetic neurons. *J Cell Biol* 154:995–1005, 2001
25. Pugazhenthi S, Nesterova A, Sable C, Heidenreich KA, Boxer LM, Heasley LE, Reusch JE: Akt/protein kinase B up-regulates Bcl-2 expression through cAMP-response element-binding protein. *J Biol Chem* 275:10761–10766, 2000
26. Delaney CL, Russell JW, Cheng HL, Feldman EL: Insulin-like growth factor-I and over-expression of Bcl-xL prevent glucose-mediated apoptosis in Schwann cells. *J Neuropathol Exp Neurol* 60:147–160, 2001
27. Putcha GV, Deshmukh M, Johnson EMJ: BAX translocation is a critical event in neuronal apoptosis: regulation by neuroprotectants, BCL-2, and caspases. *J Neurosci* 19:7476–7485, 1999
28. Easton RM, Deckwerth TL, Parsadanian AS, Johnson EMJ: Analysis of the mechanism of loss of trophic factor dependence associated with neuronal maturation: a phenotype indistinguishable from Bax deletion. *J Neurosci* 17:9656–9666, 1997
29. Patel J, Tomlinson DR: Nerve conduction impairment in experimental diabetes-proximodistal gradient of severity. *Muscle Nerve* 22:1403–1411, 1999
30. Huang TJ, Sayers NM, Fernyhough P, Verkhratsky A: Diabetes-induced alterations in calcium homeostasis in sensory neurones of streptozotocin-diabetic rats are restricted to lumbar ganglia and are prevented by neurotrophin-3. *Diabetologia* 45:560–570, 2002
31. Nicholls DG, Ward MW: Mitochondrial membrane potential and neuronal glutamate excitotoxicity: mortality and millivolts. *Trends Neurosci* 23: 166–174, 2000
32. Usachev Y, Shmigol A, Pronchuk N, Kostyuk P, Verkhratsky A: Caffeine-induced calcium release from internal stores in cultured rat sensory neurons. *Neuroscience* 57:845–859, 1993
33. Patterson GH, Knobel SM, Arkhammar P, Thastrup O, Piston DW: Separation of the glucose-stimulated cytoplasmic and mitochondrial NAD(P)H responses in pancreatic islet beta cells. *Proc Natl Acad Sci U S A* 97:5203–5207, 2000
34. Russell JW, Golovoy D, Vincent AM, Mahendru P, Olzmann JA, Mentzer A, Feldman EL: High glucose-induced oxidative stress and mitochondrial dysfunction in neurons. *FASEB J* 16:1738–1748, 2002
35. De Giorgi F, Lartigue L, Bauer MK, Schubert A, Grimm S, Hanson GT, Remington SJ, Youle RJ, Ichas F: The permeability transition pore signals apoptosis by directing Bax translocation and multimerization. *FASEB J* 16:607–609, 2002
36. Purves T, Middlemas A, Agthong S, Jude EB, Boulton AJ, Fernyhough P, Tomlinson DR: A role for mitogen-activated protein kinases in the etiology of diabetic neuropathy. *FASEB J* 15:2508–2514, 2001
37. Zochodne DW, Verge VM, Cheng C, Sun H, Johnston J: Does diabetes target ganglion neurones? Progressive sensory neurone involvement in long-term experimental diabetes. *Brain* 124:2319–2334, 2001
38. Schmidt RE, Dorsey D, Parvin CA, Beaudet LN, Plurad SB, Roth KA: Dystrophic axonal swellings develop as a function of age and diabetes in human dorsal root ganglia. *J Neuropathol Exp Neurol* 56:1028–1043, 1997
39. Whitesell RR, Ward M, McCall AL, Granner DK, May JM: Coupled glucose transport and metabolism in cultured neuronal cells: determination of the rate-limiting step. *J Cereb Blood Flow Metab* 15:814–826, 1995
40. Saltiel AR, Kahn CR: Insulin signalling and the regulation of glucose and lipid metabolism. *Nature* 414:799–806, 2001
41. Pilkis SJ, Granner DK: Molecular physiology of the regulation of hepatic gluconeogenesis and glycolysis. *Annu Rev Physiol* 54:885–909, 1992
42. Sutherland C, O'Brien RM, Granner DK: New connections in the regulation of PEPCK gene expression by insulin. *Philos Trans R Soc Lond B Biol Sci* 351:191–199, 1996
43. Gopalakrishnan L, Scarpulla RC: Differential regulation of respiratory chain subunits by a CREB-dependent signal transduction pathway: role of cyclic AMP in cytochrome c and COXIV gene expression. *J Biol Chem* 269:105–113, 1994
44. Herzig RP, Scacco S, Scarpulla RC: Sequential serum-dependent activation of CREB and NRF-1 leads to enhanced mitochondrial respiration through the induction of cytochrome c. *J Biol Chem* 275:13134–13141, 2000
45. Mayr B, Montminy M: Transcriptional regulation by the phosphorylation-dependent factor CREB. *Nat Rev Mol Cell Biol* 2:599–609, 2001
46. Wuytack F, Raeymaekers L, Missiaen L: Molecular physiology of the SERCA and SPCA pumps. *Cell Calcium* 32:279–305, 2002
47. Friel DD: Mitochondria as regulators of stimulus-evoked calcium signals in neurons. *Cell Calcium* 28:307–316, 2000
48. Lowery JM, Eichberg J, Saubermann AJ, LoPachin RM Jr: Distribution of elements and water in peripheral nerve of streptozocin-induced diabetic rats. *Diabetes* 39:1498–1503, 1990
49. Mattson MP, Barger SW, Begley JG, Mark RJ: Calcium, free radicals, and excitotoxic neuronal death in primary cell culture. *Methods Cell Biol* 46:187–216, 1995
50. Glazner GW, Fernyhough P: Neuronal survival in the balance: are endoplasmic reticulum membrane proteins the fulcrum? *Cell Calcium* 32:421–433, 2002
51. Obrosova IG, Van Huysen C, Fathallah L, Cao XC, Greene DA, Stevens MJ: An aldose reductase inhibitor reverses early diabetes-induced changes in peripheral nerve function, metabolism, and antioxidative defense. *FASEB J* 16:123–125, 2002
52. Fernyhough P, Gallagher A, Averill SA, Priestley JV, Hounsom L, Patel J, Tomlinson DR: Aberrant neurofilament phosphorylation in sensory neurons of rats with diabetic neuropathy. *Diabetes* 48:881–889, 1999
53. Tomlinson DR, Mayer JH: Defects of axonal transport in diabetes mellitus: a possible contribution to the aetiology of diabetic neuropathy. *J Auton Pharmacol* 4:59–72, 1984